BLM LIBRARY
88019632

LA-6414-MS
Informal Report

UC-91
Reporting Date: June 1976
Issued: July 1976

Electron Microprobe Studies of Mahogany Zone and Devonian Oil Shales

by

E. A. Hakkila
N. E. Elliott
J. M. Williams
E. M. Wewerka

los alamos
scientific laboratory
of the University of California
LOS ALAMOS, NEW MEXICO 87545

ve Action/Equal Opportunity Employer

AREA OIL SHALE OFFICE
CENTRAL LIBRARY

QE
471
.S5
H35
1976
c.2

UNITED STATES
ENERGY RESEARCH AND DEVELOPMENT ADMINISTRATION
CONTRACT W-7405-ENG. 36

This work was supported by the US Energy Research and Development Administration, Division of Environmental Control Technology, Contract No. IAG-D5-E681, and the Environmental Protection Agency, Industrial Environmental Research Laboratory, Research Triangle Park, NC.

Printed in the United States of America. Available from
National Technical Information Service
U.S. Department of Commerce
5285 Port Royal Road
Springfield, VA 22161
Price: Printed Copy $3.50 Microfiche $2.25

ID88019632

QE
471
.25
H35
1976
c.2

BLM Library
D-553A, Building 50
Denver Federal Center
P. O. Box 25047
Denver, CO 80225-0047

ELECTRON MICROPROBE STUDIES OF MAHOGANY ZONE AND DEVONIAN OIL SHALES

by

E. A. Hakkila, N. E. Elliott, J. M. Williams, and E. M. Wewerka

ABSTRACT

A sample of Mahogany zone oil shale from the Piceance Basin of Colorado and a sample of Devonian shale from the Marcelus Layer of West Virginia were examined with the electron microprobe. The examination results were correlated to previously published mineralogical data. The studies showed that many mineral identifications could be obtained from elemental associations without resorting to complete quantitative mineral analyses.

I. INTRODUCTION

Two samples of oil shale have been examined with the electron microprobe to measure distributions of several elements in various layers and to identify minerals present. One sample consisted of Mahogany zone shale from the Piceance Basin of Colorado, the second sample was Devonian shale from the 800-m depth of the Marcelus Layer, Consolidated Gas Well No. 9041, Jackson County, West Virginia. For electron microprobe analyses, the samples were slabbed to obtain a piece approximately 2.5 cm long and 1.2 cm wide. The samples were metallographically polished to reveal the microstructure, and were coated with a layer of carbon approximately 100 Å thick to provide electrical conductivity. The Mahogany zone shale exhibited distinctive light and dark bands; bands were less pronounced in the Devonian shale.

The electron microprobe has been applied in numerous instances to quantitative identification of mineral species.[1,2] Generally, intensities of characteristic x rays for the elements of interest are measured from the unknown and from pure end member oxides, and intensity ratios are converted to weight fractions using empirically determined correction parameters.[3,4] This technique generally provides quantitative analyses accurate to 1 to 5% relative of the amount present for major constituents.

In many cases some mineral identifications can be obtained from a knowledge of the mineralogy of the sample of interest and from information on elemental associations. Much information is available on the mineralogy of oil shales and particularly the Mahogany shale of the Piceance Basin.[5] With this information, the electron microprobe can provide a rapid semiquantitative identification of mineral components in the various shale layers.

II. INSTRUMENTATION

The instrument used in this study was an Applied Research Laboratories electron microprobe, Model EMX-SM, equipped with three spectrometers each having two crystals. The crystals available, LiF, ADP, RAP, and PbST, covered the wavelength region from 1.1 to 100 Å and provided capability to measure all elements of Z=5 (boron) or greater. The x-ray spectrometers, stage motion in the x- and y-directions, and scaler-timer readout could be controlled with a PDP-8E computer. A secondary electron detector provided capability to obtain scanning electron micrographs showing surface topology which could be compared with photomicrographs and two-dimensional x-ray images to correlate elemental distributions with surface features.

III. ANALYTICAL RESULTS

A. Mahogany Zone Shale

The banding in the Mahogany zone shale is clearly shown in the photomicrograph, Figure 1. Areas of specific interest that were examined in more detail included: the dark bands containing metallic-appearing inclusions (Area A); the brown band through the center of the sample containing a longitudinal crack (Area B); and the dark black band near one edge of the sample (Area C). The following elements were sought in each area,but unless otherwise noted, were not detected: C, O, Na, Mg, Al, Si, P, S, Cl, K, Ca, Ti, Cr, Mn, Fe, Ni, Cu, Zn, As, Se, Br, Zr, Nb, Mo, Rh, Ag, Cd, Sn, Sb, Ta, W, Hg, Pb, Bi, Th, and U. Detection limits were estimated to be in the range between 0.01 and 1 percent, and depended on the element and whether photographic or counting techniques were used.

1. Area A

The metallic-appearing particles appear as light, often angular, crystals in the scanning electron micrograph, Figure 2a. They contain only S (Figure 2b) and Fe (Figure 2c) in detectable concentrations, and probably are pyrite or marcasite. At least three other mineral phases are present in this area. A phase that appears fine grained in Figure 2a contains predominantly Ca (Figure 2d), Mg (Figure 2e), C (Figure 2f), and O (Figure 2k), and small amounts of Fe. This probably is a dolomite. A phase that appears as large circular grains in Figure 2a contains predominantly Al (Figure 2g), Na (Figure 2h), Si (Figure 2i), and O. This may be albite. K (Figure 2j) appears to be more closely associated with

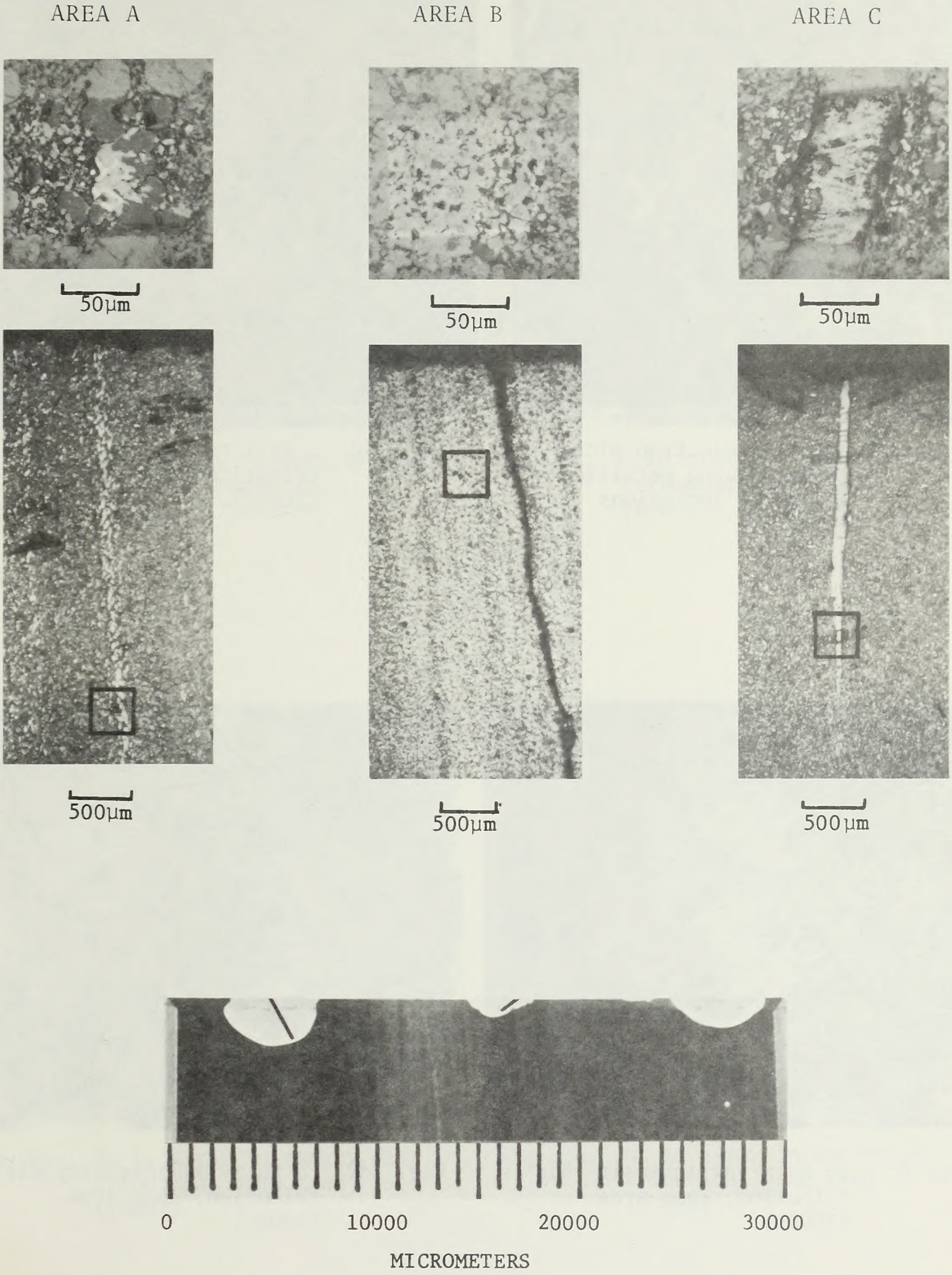

Fig. 1. Photomicrograph showing Mahogany zone shale, 3.3x. Upper photos show detail of areas examined with the microprobe.

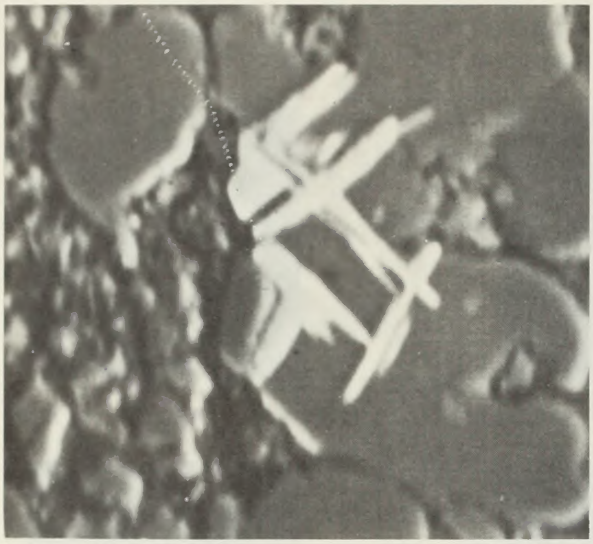

Fig. 2a. Scanning electron micrograph showing metallic-appearing inclusions (1000x).

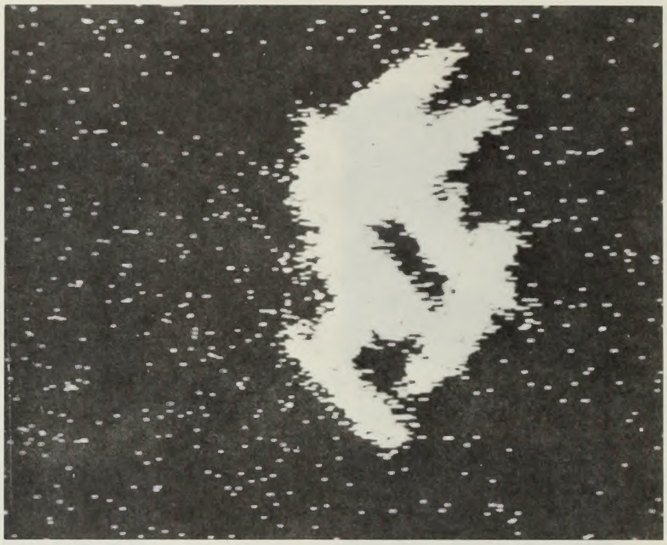

Fig. 2b. S Kα x-ray intensity distribution, same area (1000x).

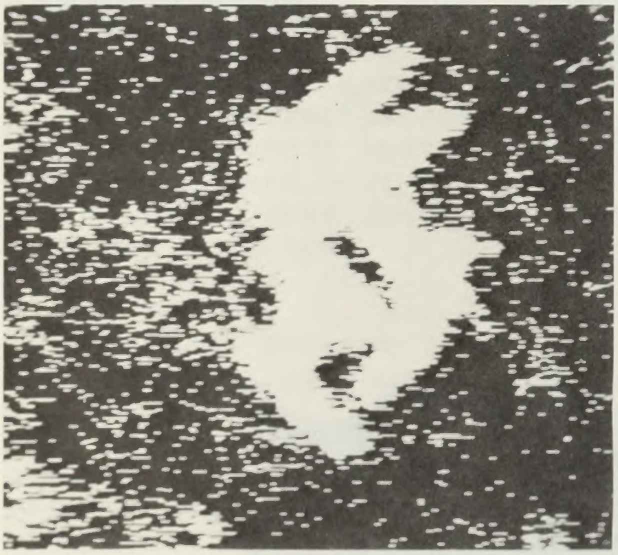

Fig. 2c. Fe Kα x-ray intensity distribution, same area (1000x).

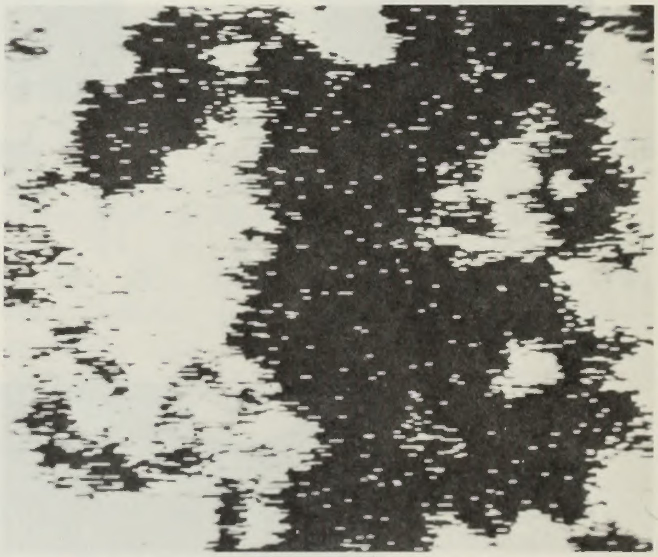

Fig. 2d. Ca Kα x-ray intensity distribution, same area (1000x).

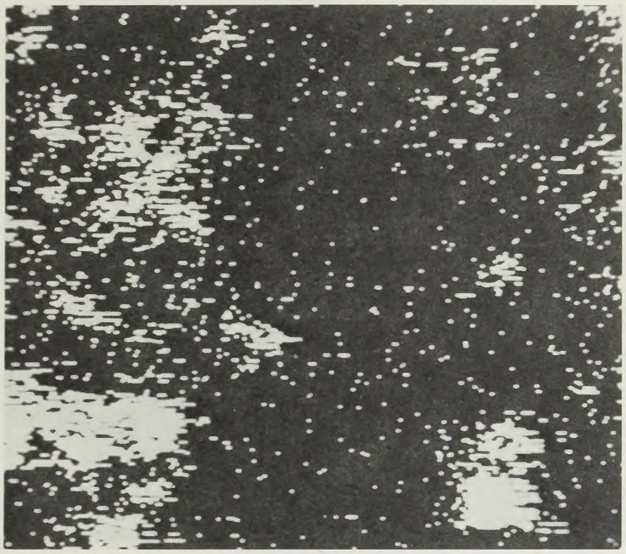

Fig. 2e. Mg Kα x-ray intensity distribution, same area (1000x).

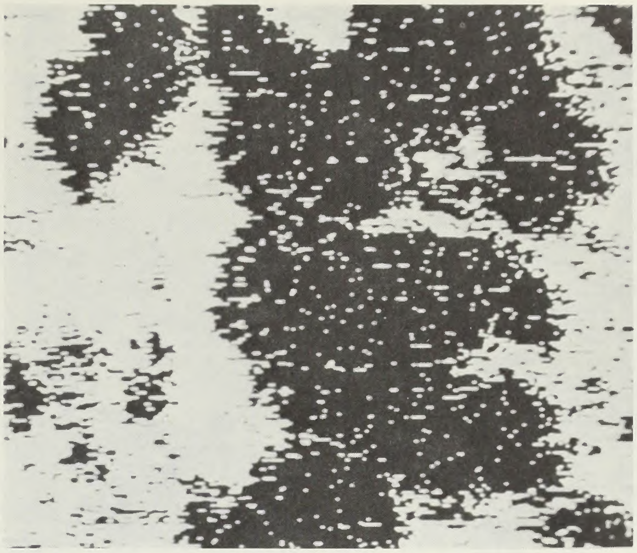

Fig. 2f. C Kα x-ray intensity distribution, same area (1000x).

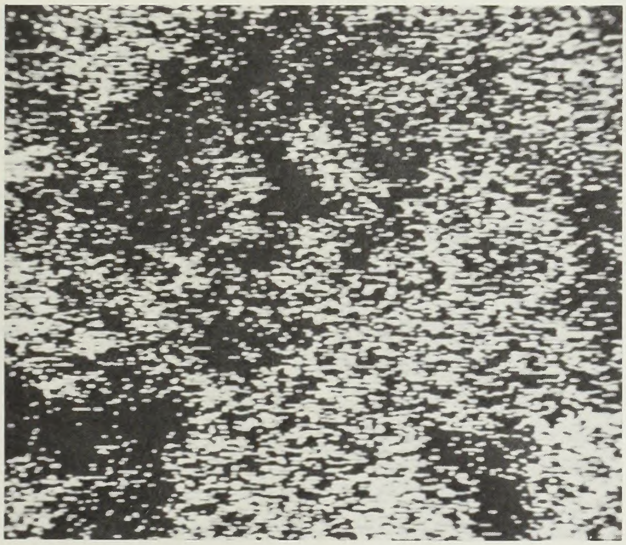

Fig. 2g. Al Kα x-ray intensity distribution, same area (1000x).

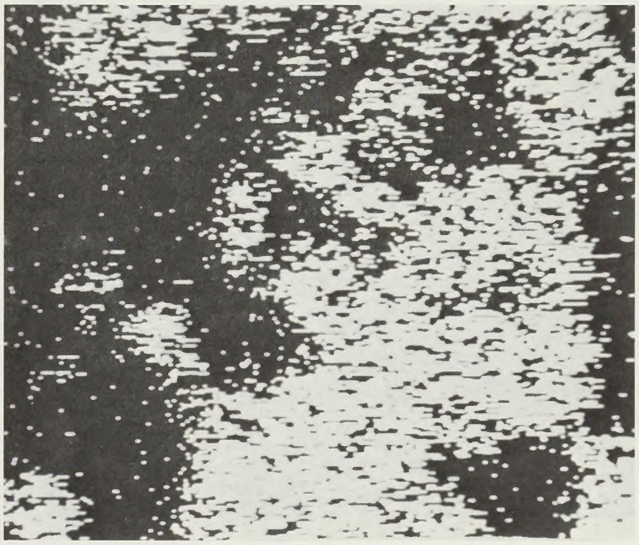

Fig. 2h. Na Kα x-ray intensity distribution, same area (1000x).

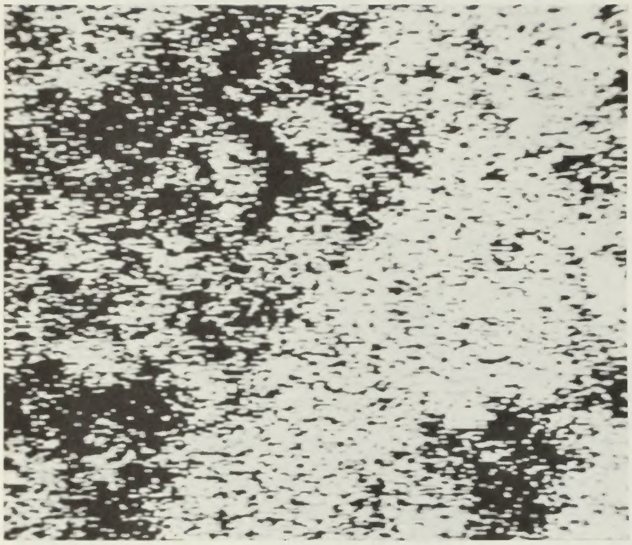

Fig. 2i. Si Kα x-ray intensity distribution, same area (1000x).

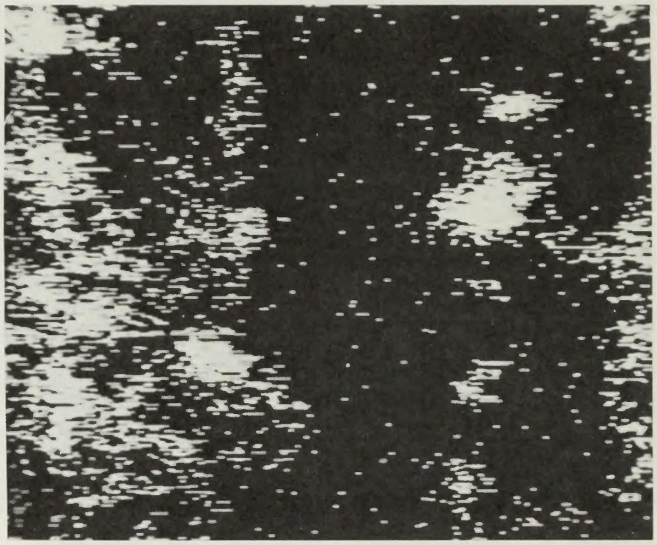

Fig. 2j. K Kα x-ray intensity distribution, same area (1000x).

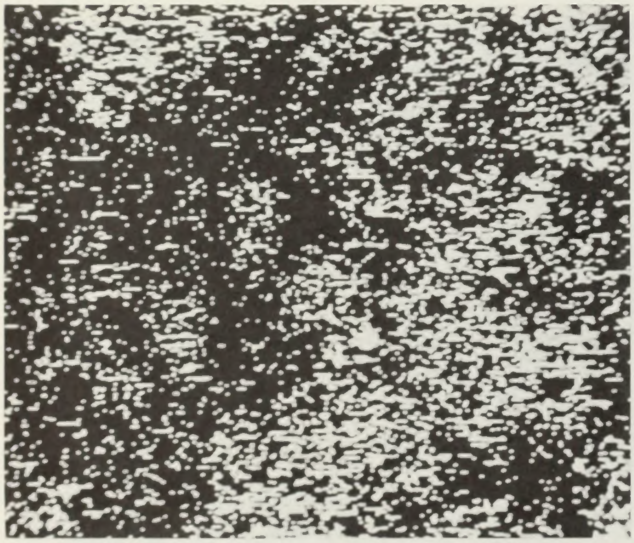

Fig. 2k. O Kα x-ray intensity distribution, same area (1000x).

the carbonate rather than the silicate phases, but the grain size is too small for proper verification. Ti (no figure) also is present in small inclusions, but the association of Ti is not apparent.

2. Area B

Area B is a light brown strip on either side of the crack near the center of the sample. A typical location in this area is shown in the scanning electron micrograph, Figure 3a. The area is characterized by a significantly higher Fe concentration than the darker areas of the sample (Figure 3b), with the Fe associated with Mg (Figure 3c), Ca (no figure), C (Figure 3d), and O (no figure). This material probably is an Fe-rich dolomite. Between grains of this material is a mineral that contains predominantly Al (Figure 3e), K (Figure 3f), Si (Figure 3g), and O. This may be illite. The mineral at the extreme lower right in Figure 3 containing Al and Si without K possibly is a kaolin mineral. Note the quartz grain at the center of Figure 3. A small grain that appears as a light inclusion near the upper center of Figure 3a contains Ti (Figure 3h) and O, and probably is rutile.

3. Area C

Area C contains a black strip that appears as a low-density phase in the scanning electron micrograph, Figure 4a. Low-density materials have a low secondary electron emission, hence the dark color on scanning electron micrographs. This strip contains predominantly C (Figure 4b) but with significant amounts of Na (Figure 4c), S (Figure 4d), and O (no figure). The S probably is organic, as indicated by the shape of the Kβ bands.[6]

A dolomite phase containing less Fe and Mg than in Area B and a silicate phase containing Ca, Al, and K are heterogeneously distributed around the C-rich band. Small inclusions, generally less than 5 μm in diameter, that contain Ti and O are present in this area.

4. Microprobe Logging and General Observations

The distributions of Fe, S, Al, Ca, and C were measured at 200-μm intervals along the length of the sample. In this analysis the electron beam was rastered rapidly over an 80- by 100-μm-square area to average the intensities over the various phases present at each location. The intensity ratios of Fe relative to pure Fe, S relative to pyrite, Al relative to pure Al, Ca relative to grossularite containing 37.2% Ca, and C relative to graphite were calculated. The intensity ratios are plotted versus position along the scans (Figure 5), and the distances shown on the scan can be correlated to distances shown in Figure 1. The analyses show, for example, that the light-tan, Fe-rich bands contain less S and Al than the darker C-rich bands. Although the light tan is basically a carbonate, the low C x-ray intensity indicated this phase is depleted in organic matter. The presence of high S concentrations in the black carbonaceous band near the 16 000-μm position also is shown. This is the same band shown in detail in Figure 4. The minerals associated with the C-rich band, the silicate areas, and the carbonate areas are in basic agreement with mineralogical data reported by Smith.[5]

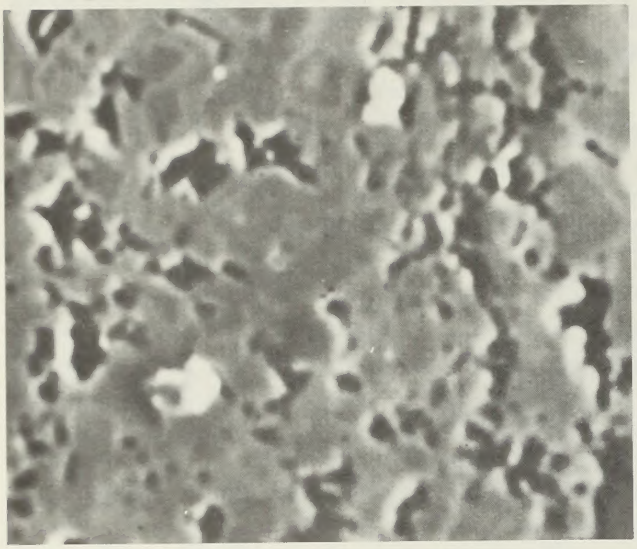

Fig. 3a. Scanning electron micrograph showing area in brown band near crack (1000x).

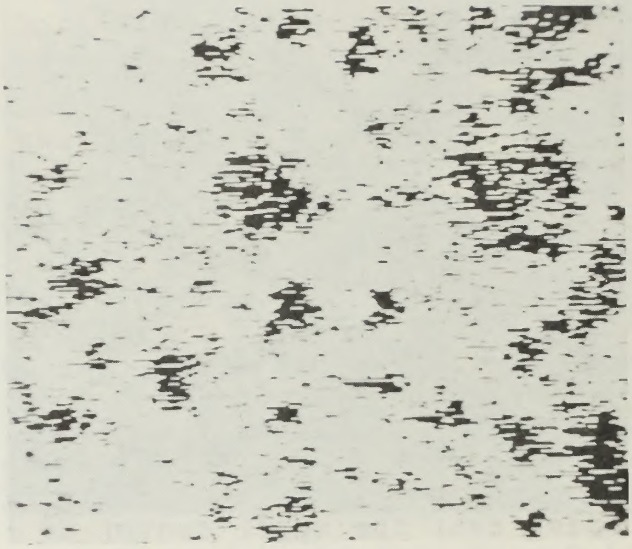

Fig. 3b. Fe Kα x-ray intensity distribution, same area (1000x).

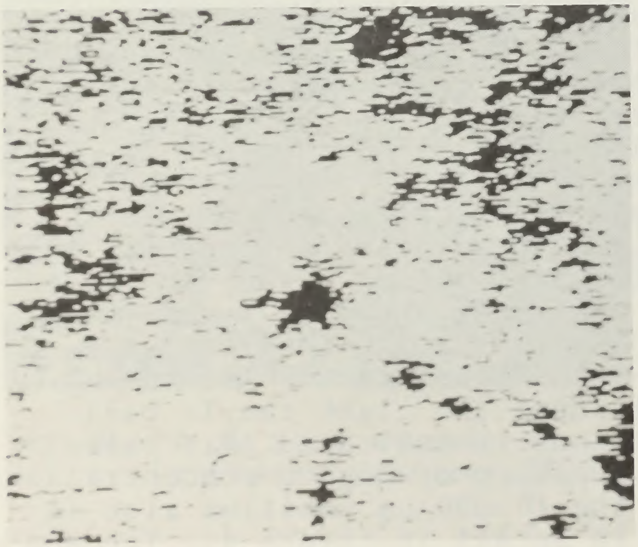

Fig. 3c. Mg Kα x-ray intensity distribution, same area (1000x).

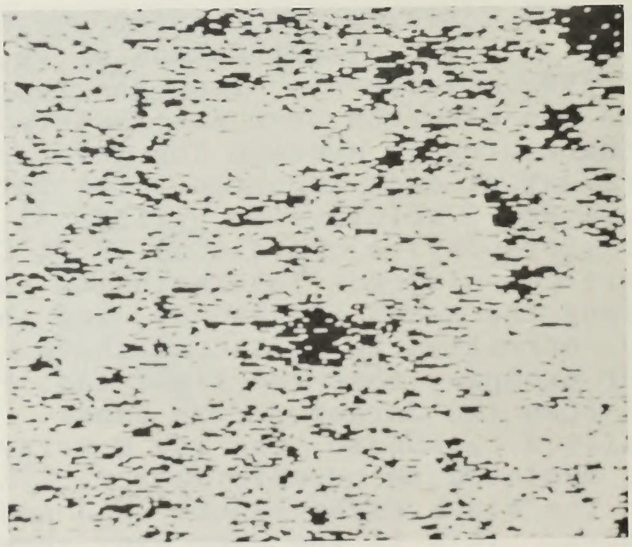

Fig. 3d. C Kα x-ray intensity distribution, same area (1000x).

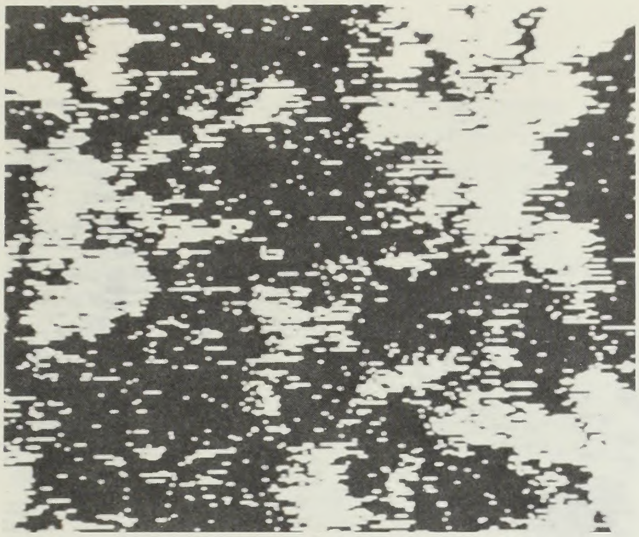

Fig. 3e. Al Kα x-ray intensity distribution, same area (1000x).

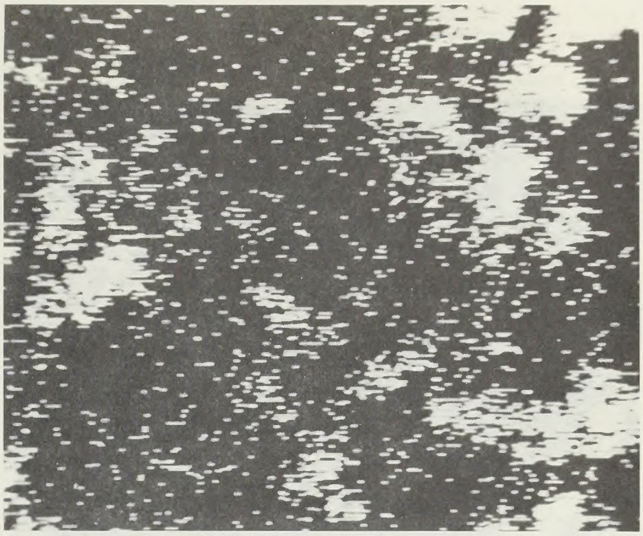

Fig. 3f. K Kα x-ray intensity distribution, same area (1000x).

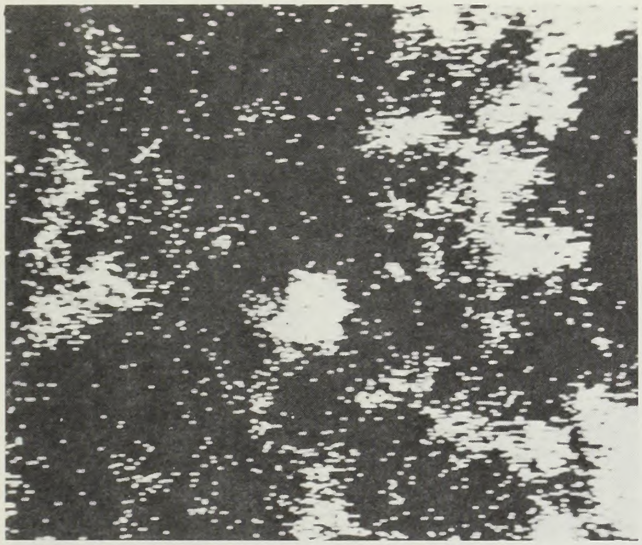

Fig. 3g. Si Kα x-ray intensity distribution, same area (1000x).

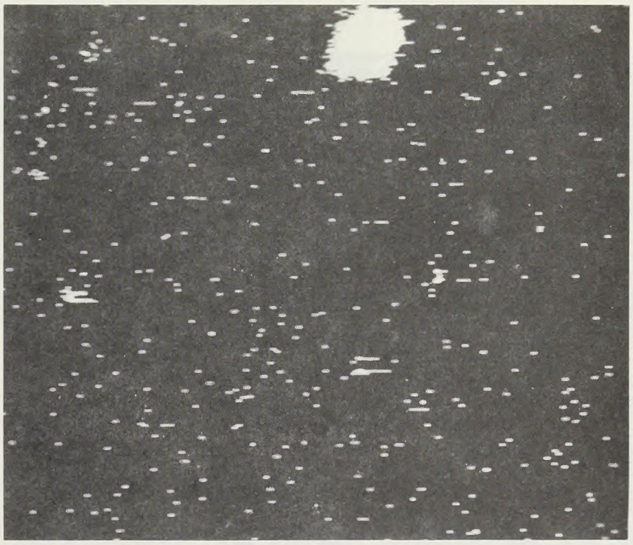

Fig. 3h. Ti Kα x-ray intensity distribution, same area (1000x).

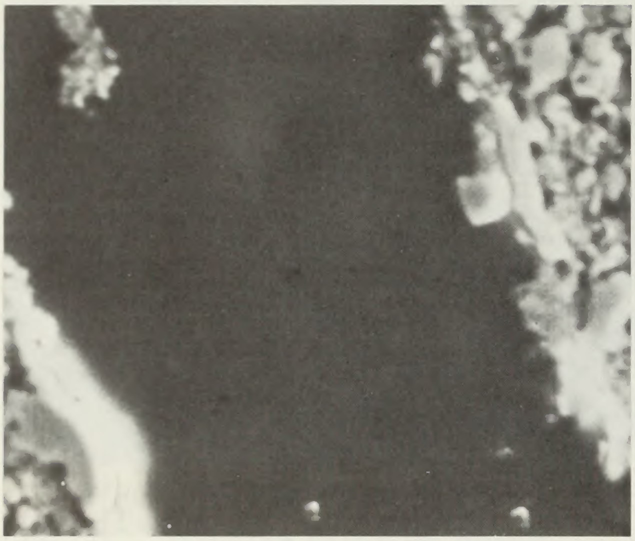

Fig. 4a. Scanning electron micrograph showing dark band near edge of sample (1000x).

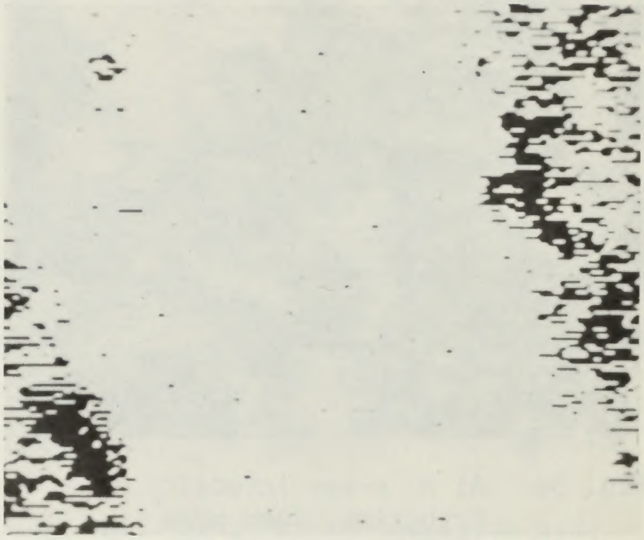

Fig. 4b. C Kα x-ray intensity distribution, same area (1000x).

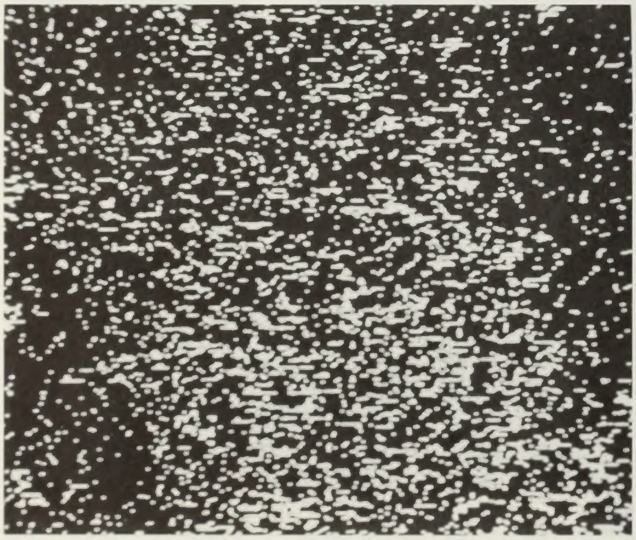

Fig. 4c. Na Kα x-ray intensity distribution, same area (1000x).

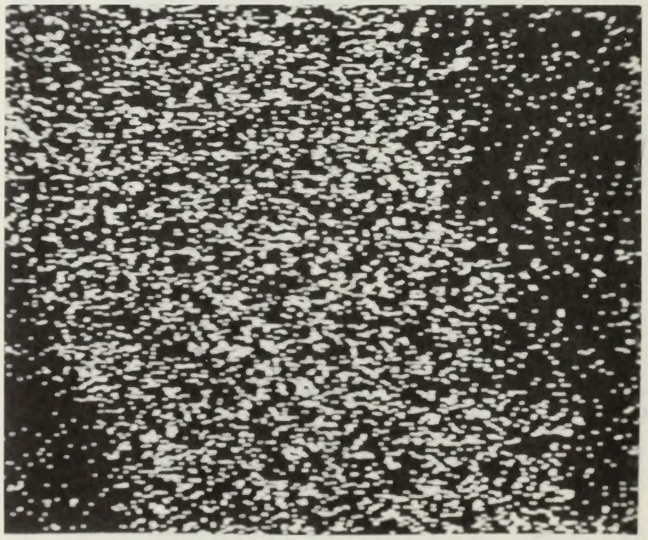

Fig. 4d. S Kα x-ray intensity distribution, same area (1000x).

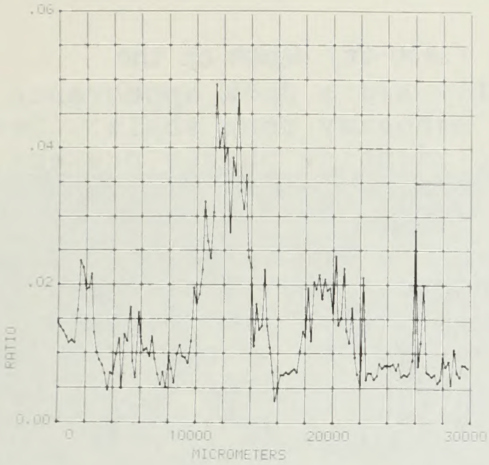

Fe Kα

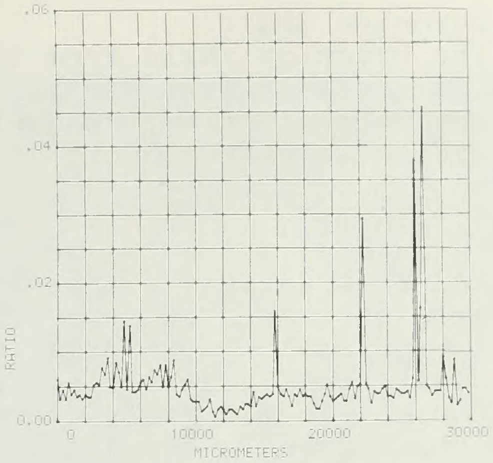

S Kα

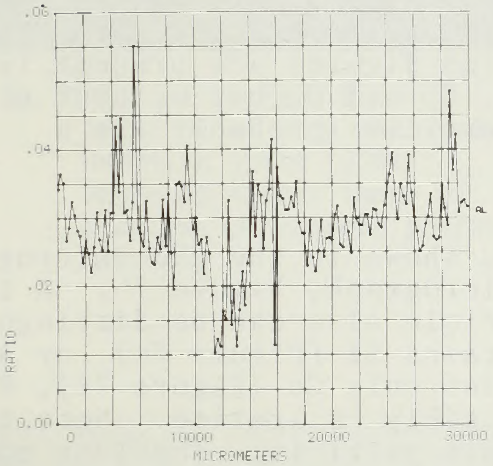

Al Kα

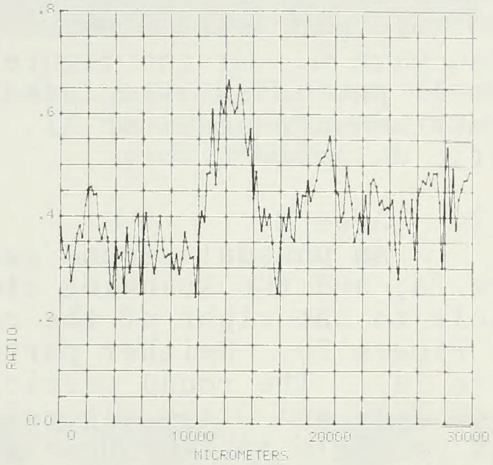

Ca Kα

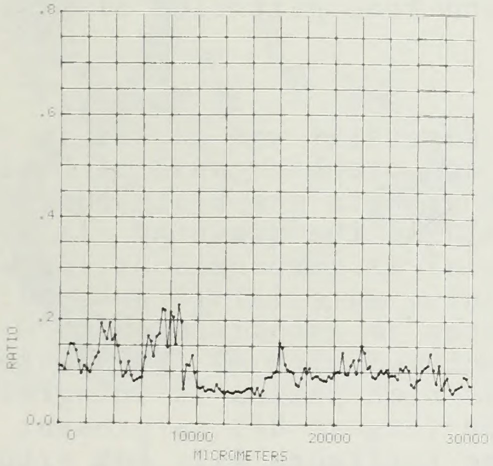

C Kα

Fig. 5. Distributions of Fe, S, Al, Ca, and C along length of Mahogany zone shale, same sample as shown in Fig. 1.

B. Devonian Shale

The Devonian shale from the 800-m (2400-ft) depth of the Marcelus Layer in West Virginia generally had a dark appearance but fewer and less distinct bands than the Mahogany zone shale. Several areas of interest were examined to identify phases present.

1. Area A

Numerous white, metallic-appearing precipitates or particles and dark phases were observed throughout the sample, and a typical area showing both types of material is shown in the photomicrograph, Figure 6a. The organic phase is clearly seen as the dark horseshoe-shaped band in the scanning electron micrograph, Figure 6b. The matrix generally contains Si (Figure 6c), Al (Figure 6d), and O (no figure). The organic phase is predominantly C (Figure 6e) and probably is organic. The metallic-appearing particles contain Fe (Figure 6f) and S (Figure 6g) and are pyrite or marcasite. An unusual irregularly shaped particle at the upper left contains predominantly Ti (Figure 6h) and C with small amounts of Fe. This is the only particle observed in which Ti is associated with C rather than with O. Mg (no figure) and C (no figure) are present in a few small particles associated with Fe, C, and O, but without significant amounts of Si or Al. These particles probably are a ferritic dolomite.

2. Area B

An unusual round particle is shown in the photomicrograph, Figure 7a, and the scanning electron micrograph, Figure 7b. A long particle to the right of the round particle also can be distinguished in Figure 7b. Neither particle contains Si (Figure 7c) or Al (Figure 7d). The round particle contains only Ca (Figure 7f), P (Figure 7g), and O (no figure), and possibly is apatite. Note the quartz particle to the upper left of this particle. The long particle is predominantly C (Figure 7e). Note that low concentrations of Ca also are present in the long carbonaceous particle. Mg (Figure 7h) and K (no figure) are present at low concentrations in some of the Al silicate phase. Small TiO_2 and FeS_2 particles also are present in this area.

3. Area C

As noted before, this sample generally was darker in appearance than the Mahogany zone shale, and black organic-rich bands were more difficult to distinguish. An area in one black band is shown in the photomicrograph, Figure 8a, and the scanning electron micrograph, igure 8b. The black material is carbonaceous (Figure 8c). This area contains more Si-containing material (Figure 8d) than the bulk of the sample. The Si often is associated with O (no figure) as quartz, but also is associated with Al (Figure 8e) and O. The higher Si content in organic-rich phases is in agreement with theory proposed by Smith.[5] Fe (Figure 8f) is present with Ca (Figure 8g), Mg (Figure 8h), and some K (Figure 8i), but without Na (Figure 8j). The Fe content is much greater, and Ca and Mg contents much lower, than in normal dolomite grains in other areas of the sample. K also is absent in normal dolomite. This material may

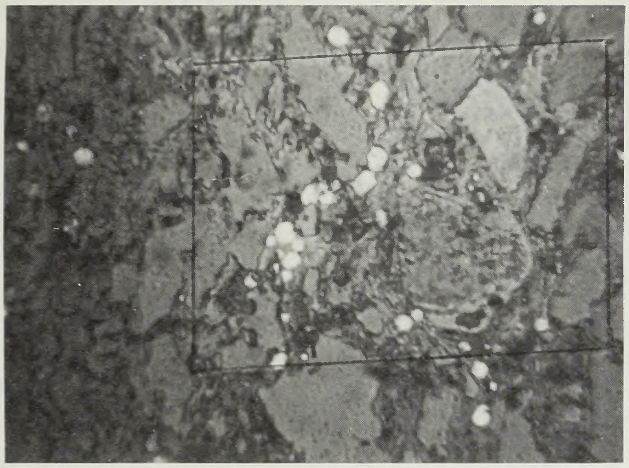

Fig. 6a. Photomicrograph showing location of area analyzed, Devonian shale (550x). Photo is mirror image of electron microprobe photos.

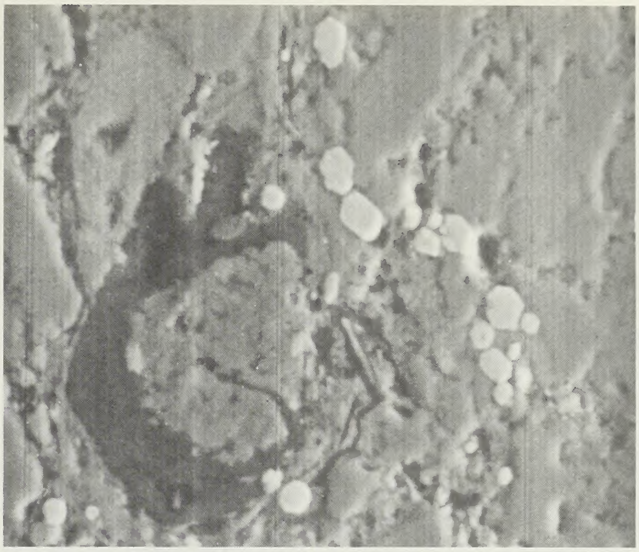

Fig. 6b. Scanning electron micrograph showing detail of area analyzed (1000x).

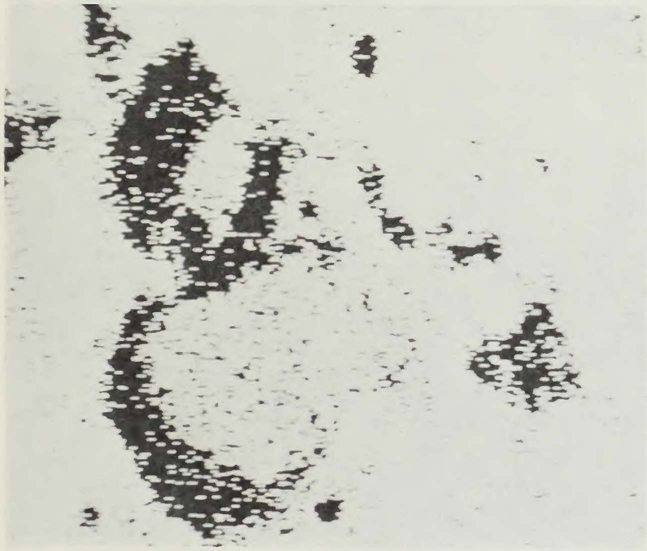

Fig. 6c. Si Kα x-ray intensity distribution, same area as shown in Fig. 6b (1000x).

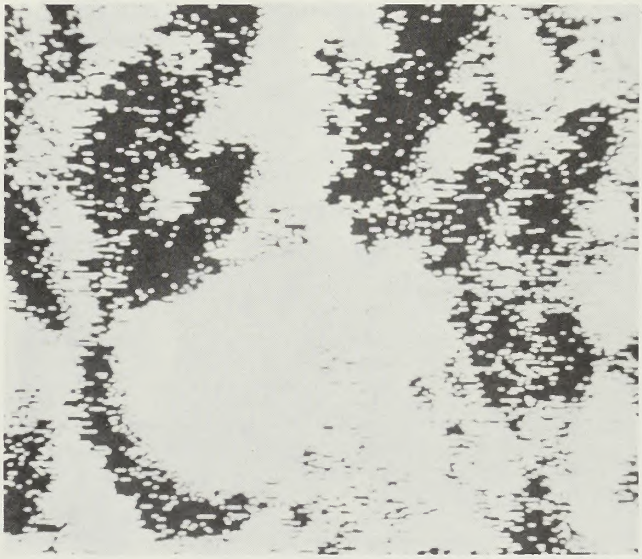

Fig. 6d. Al Kα x-ray intensity distribution, same area (1000x).

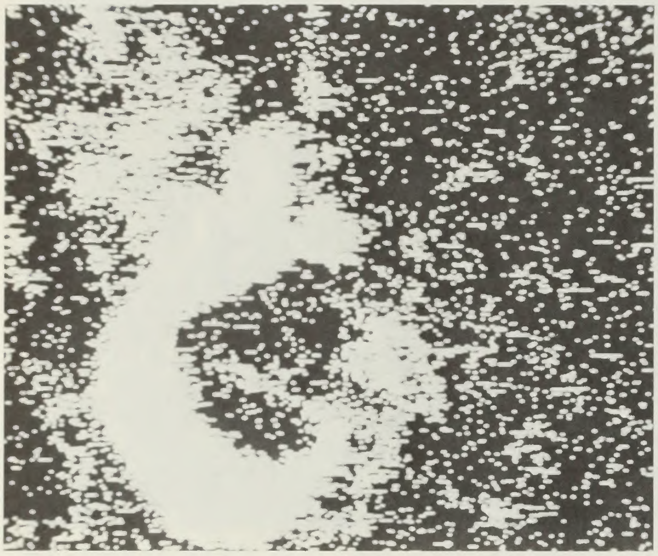

Fig. 6e. C Kα x-ray intensity distribution, same area (1000x).

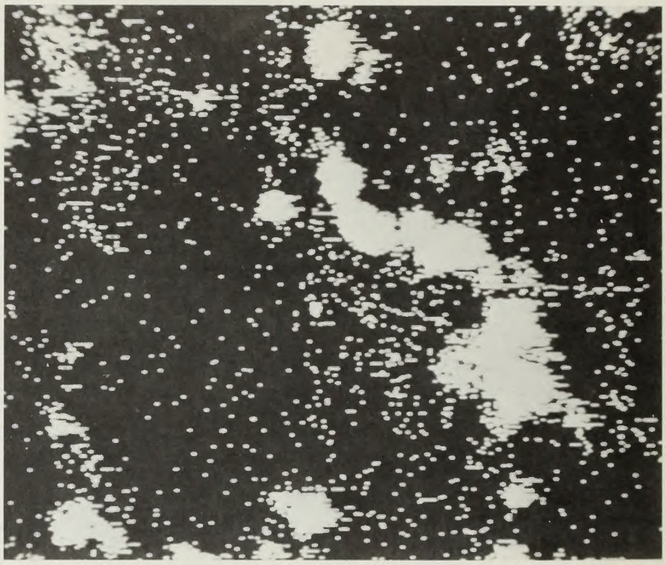

Fig. 6f. Fe Kα x-ray intensity distribution, same area (1000x).

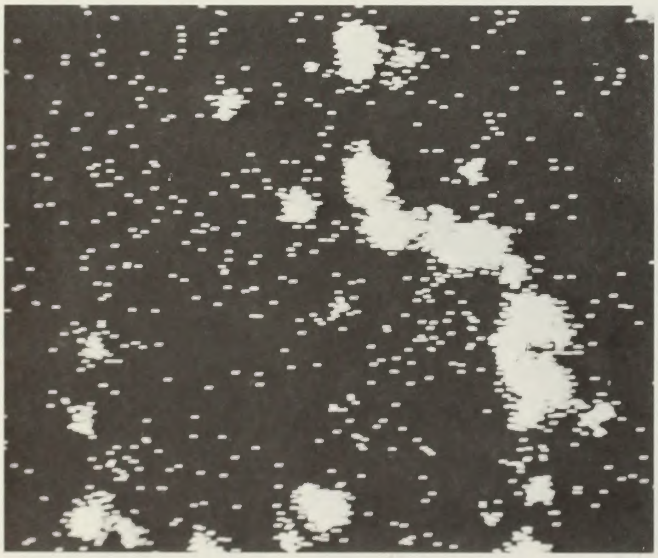

Fig. 6g. S Kα x-ray intensity distribution, same area (1000x).

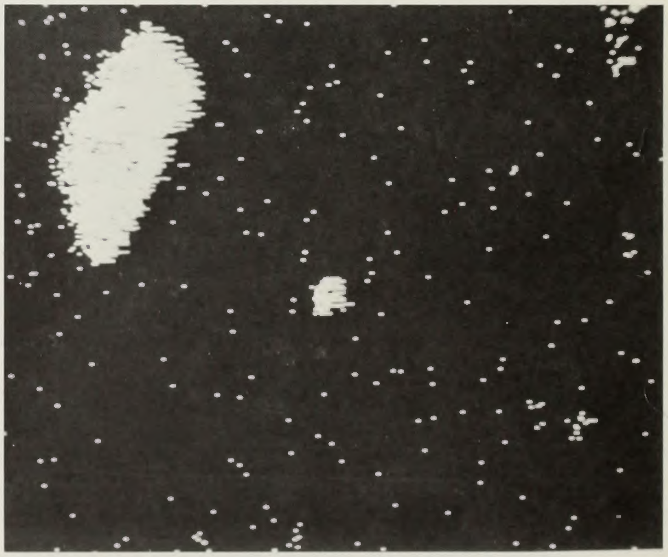

Fig. 6h. Ti Kα x-ray intensity distribution, same area (1000x).

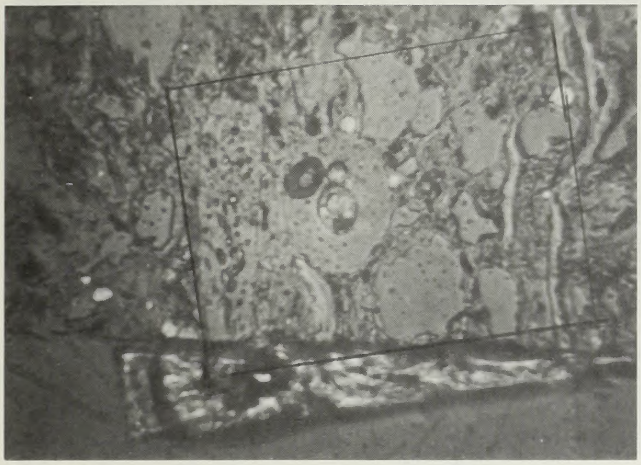

Fig. 7a. Photomicrograph showing circular particle in Devonian shale (550x). Photo is mirror image of electron microprobe photos.

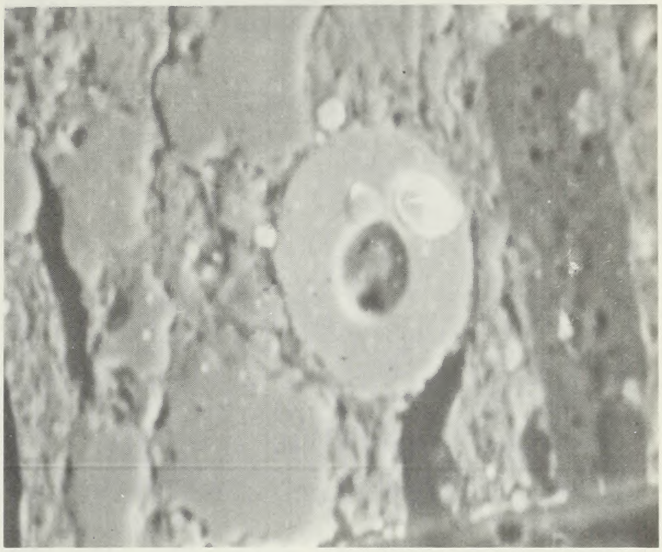

Fig. 7b. Scanning electron micrograph showing same area as shown in Fig. 7a (1000x). Also note long particle to right of circular particle.

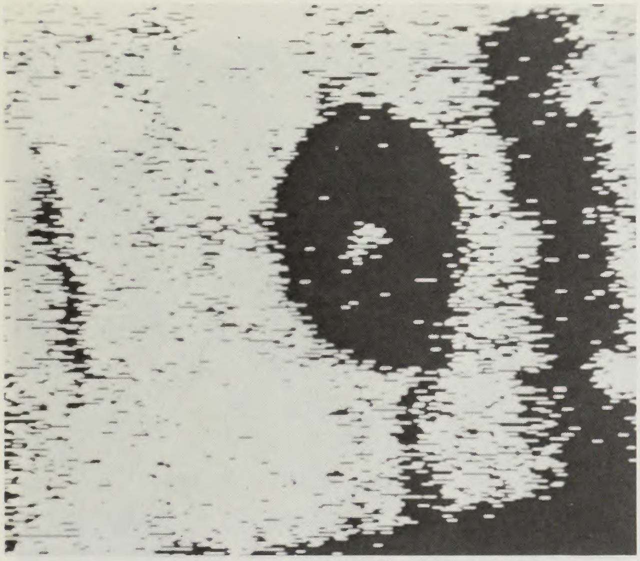

Fig. 7c. Si Kα x-ray intensity distribution, same area as shown in Fig. 7b (1000x).

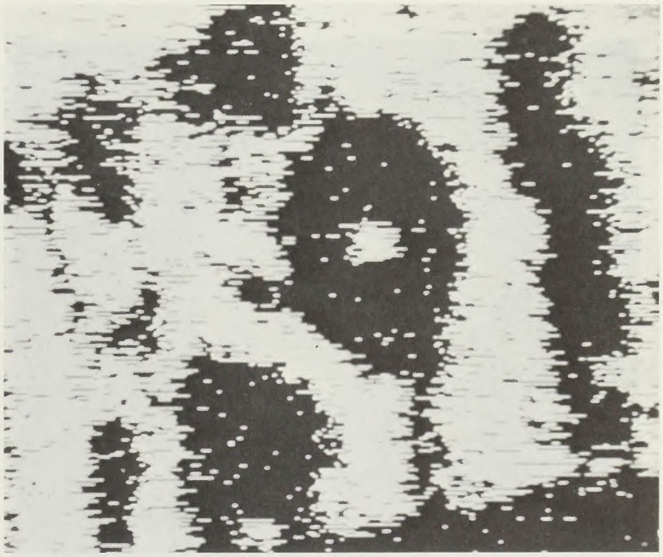

Fig. 7d. Al Kα x-ray intensity distribution, same area (1000x).

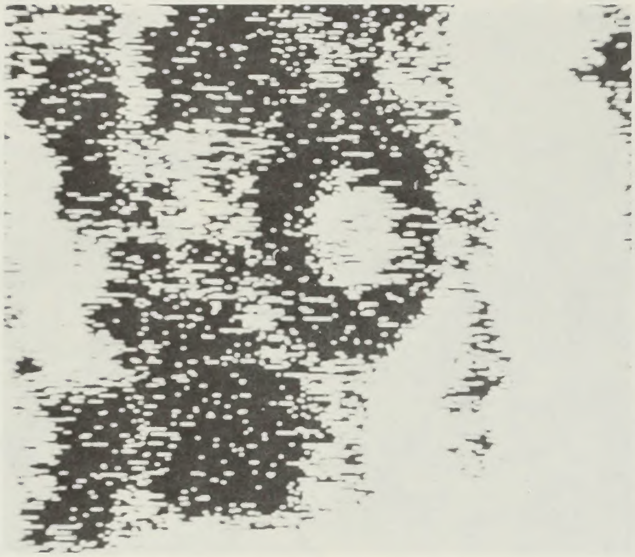

Fig. 7e. C Kα x-ray intensity distribution, same area (1000x).

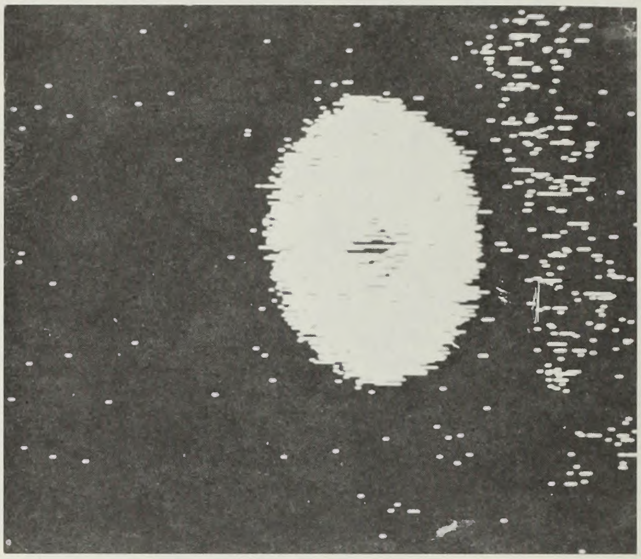

Fig. 7f. Ca Kα x-ray intensity distribution, same area (1000x).

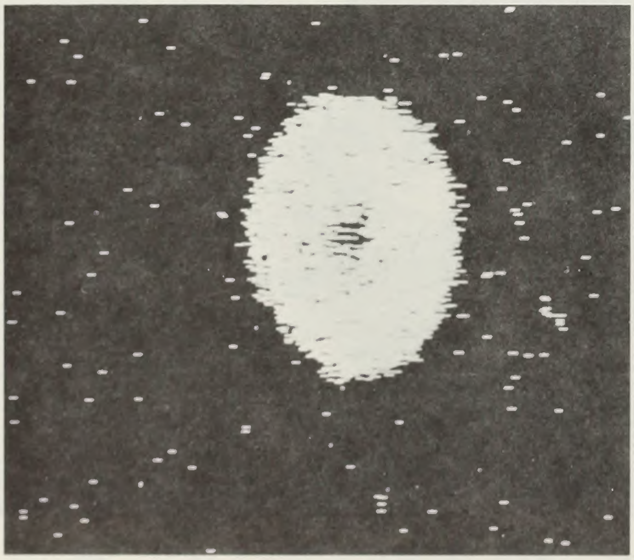

Fig. 7g. P Kα x-ray intensity distribution, same area (1000x).

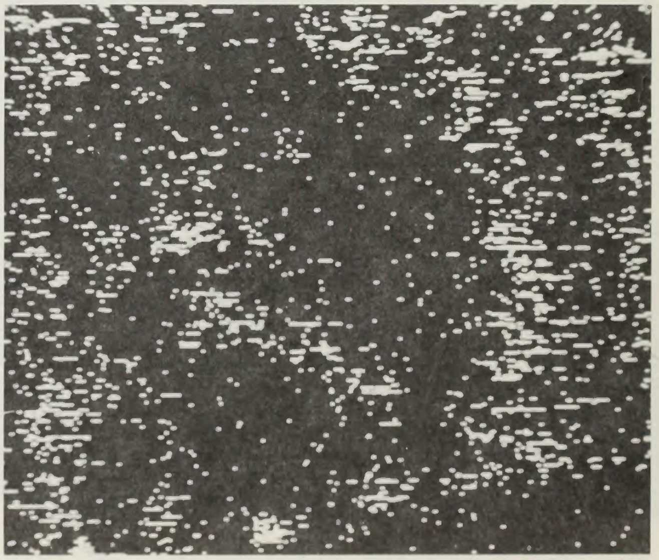

Fig. 7h. Mg Kα x-ray intensity distribution, same area (1000x).

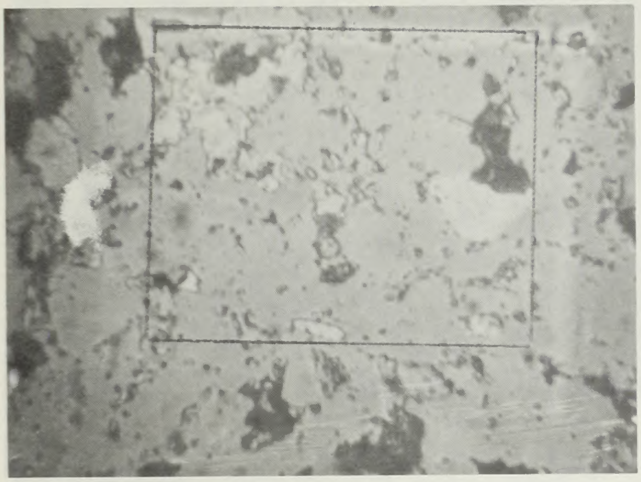

Fig. 8a. Photomicrograph showing typical area in dark band through Devonian shale (500x). Photo is mirror image of microprobe photos.

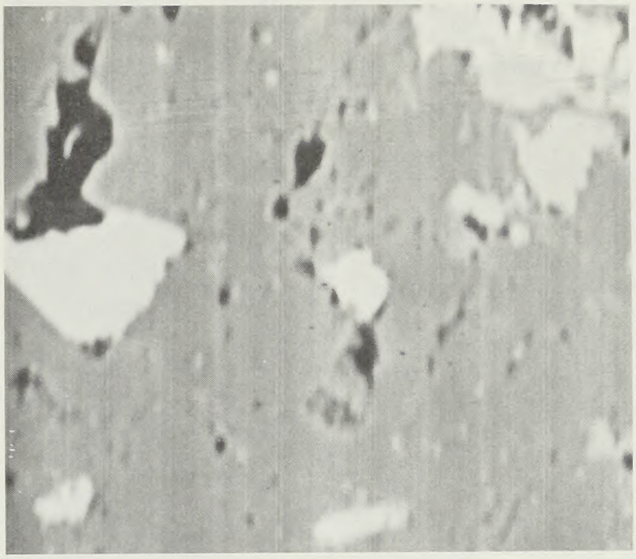

Fig. 8b. Scanning electron micrograph showing detail of area shown in Fig. 8a (1000x).

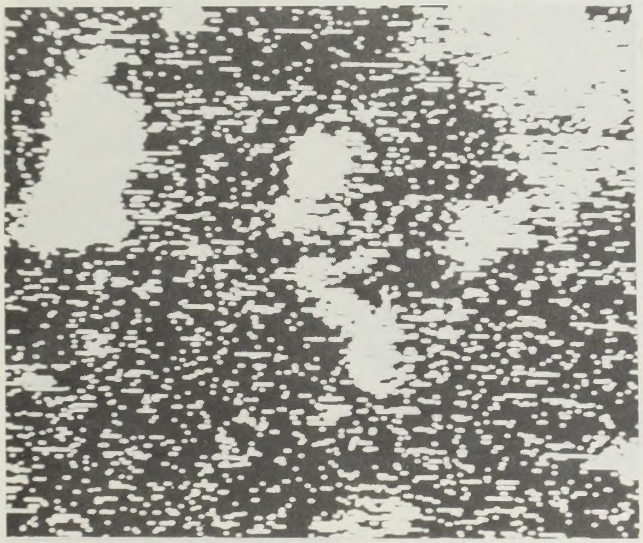

Fig. 8c. C Kα x-ray intensity distribution, same area as shown in Fig. 8b (1000x).

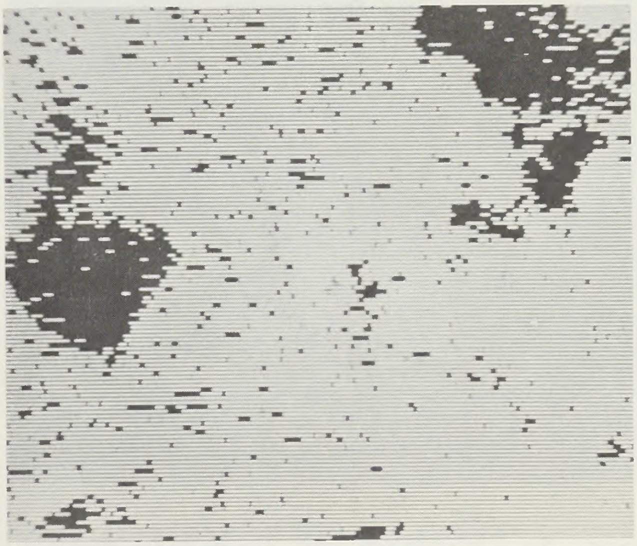

Fig. 8d. Si Kα x-ray intensity distribution, same area (1000x).

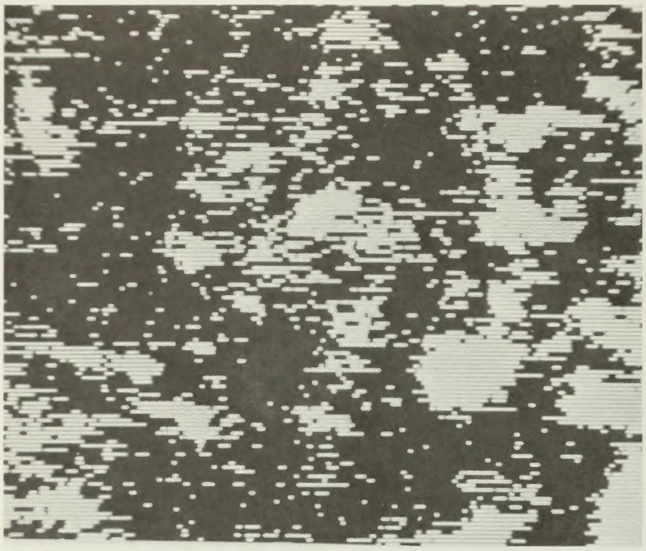

Fig. 8e. Al Kα x-ray intensity distribution, same area (1000x).

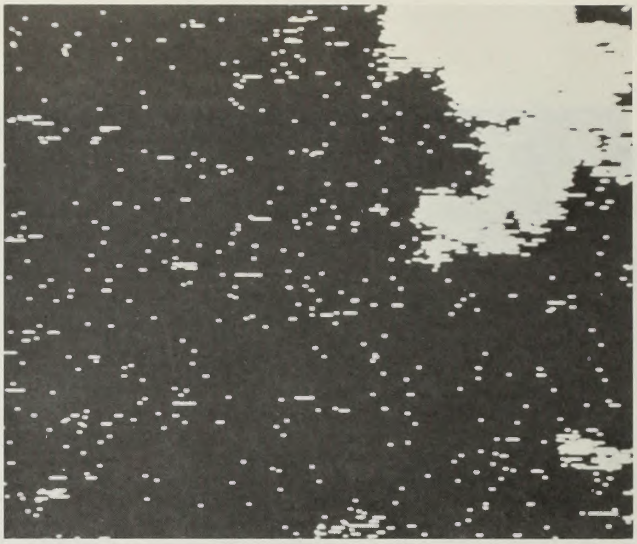

Fig. 8f. Fe Kα x-ray intensity distribution, same area (1000x).

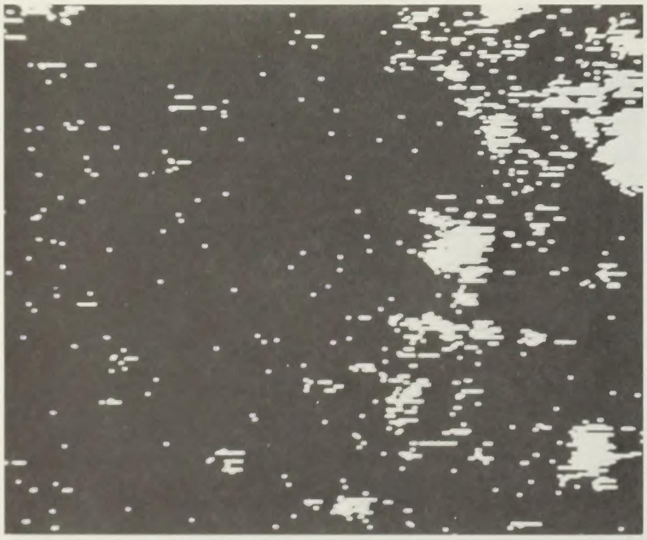

Fig. 8g. Ca Kα x-ray intensity distribution, same area (1000x).

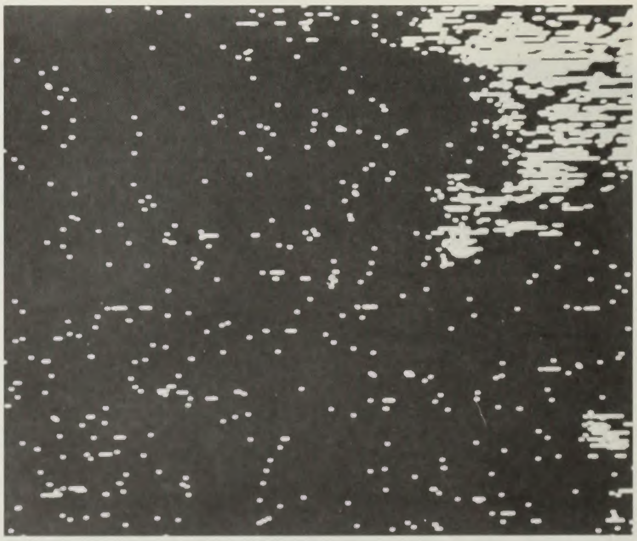

Fig. 8h. Mg Kα x-ray intensity distribution, same area (1000x).

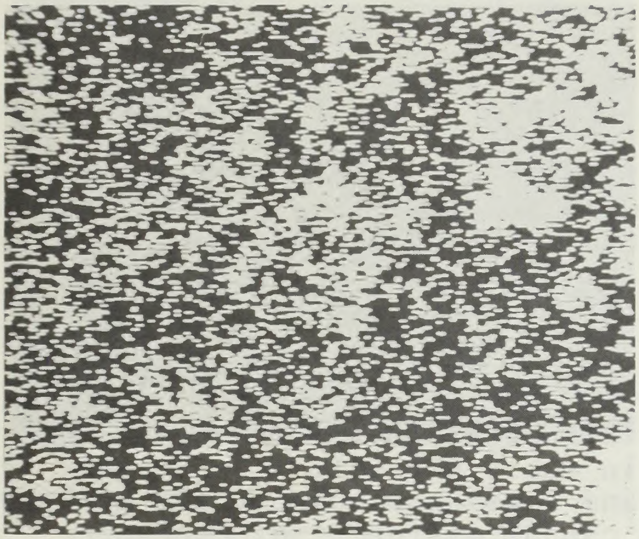

Fig. 8i. K Kα x-ray intensity distribution, same area (1000x).

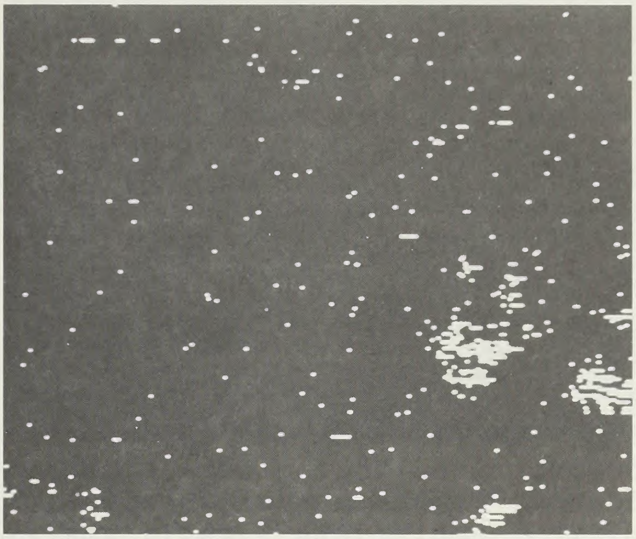

Fig. 8j. Na Kα x-ray intensity distribution, same area (1000x).

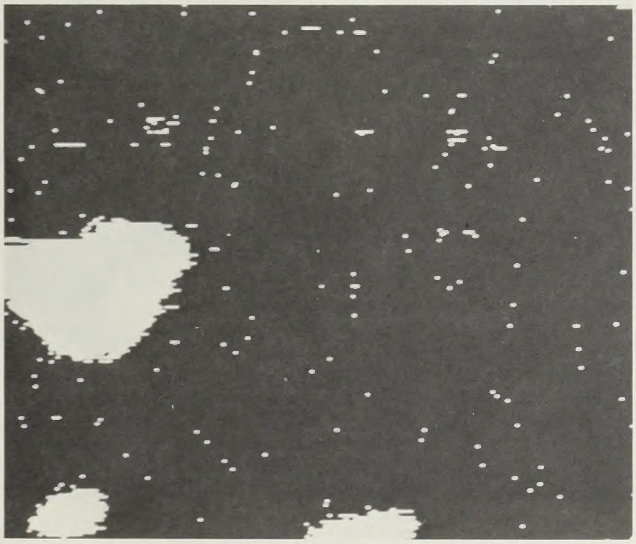

Fig. 8k. Ti Kα x-ray intensity distribution, same area (1000x).

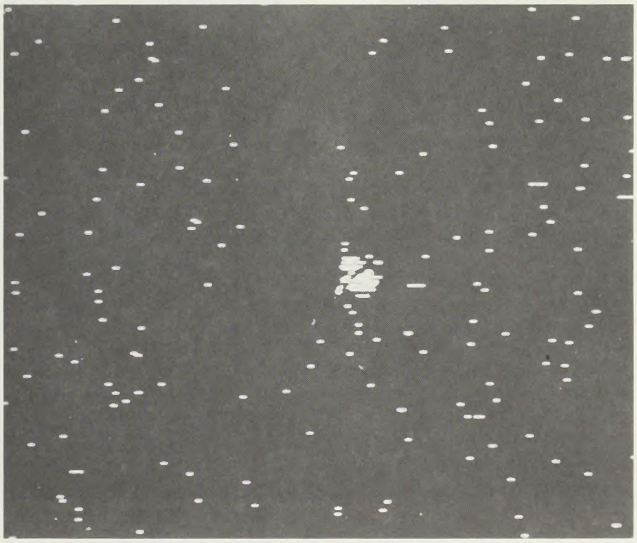

Fig. 8l. P Kα x-ray intensity distribution, same area (1000x).

be siderite rather than dolomite. The light metallic-appearing particles contain Ti (Figure 8K) and O, probably as rutile. P (Figure 8l) is present in one small inclusion, but elements associated with it are difficult to establish.

4. Area D

This sample, after polishing, was covered with a cap plug, and when the cap was removed small droplets of liquid were observed on the surface. On exposure to air the liquid disappeared. Small cubic crystals (Figures 9a, 9b) containing Na (Figure 9c) and Cl (Figure 9d) were observed on the sample surface. These NaCl crystals probably formed after sample preparation, and were left as deposits after evaporation of the liquid.

IV. CONCLUSIONS

The electron microprobe study, although limited in scope, has demonstrated that minerals present in small particles can be inferred from elemental associations and some knowledge of the history of the sample. This rapid analysis cannot differentiate between similar species such as pyrite-marcasite (FeS_2), or rutile-brookite-octahedrite (TiO_2). However, a quantitative microprobe analysis cannot differentiate these species either, and x-ray diffraction analysis is required. If the microprobe studies are performed in conjunction with x-ray diffraction studies, the need for more complex quantitative microprobe analysis could be significantly minimized, although not eliminated completely.

The analyses of these samples show that, in both types of shale, silicate phases predominate in the organic-rich areas, whereas carbonates are more prevalent in the organic-poor areas. This observation is in agreement with mineralogical studies of similar samples. The Mahogany zone shale has more illite than the Devonian shale, indicating the Mahogany shale was formed at a higher pH. The presence of siderite in the Devonian shale also is indicative of lower pH, that is, the availability of Fe^{++} in excess of available $CaCO_3$. Another notable difference between the two shale samples is the presence of significant amounts of S in the organic material in the Mahogany shale and almost complete absence of S in the organic matter of the Devonian shale.

Obviously, these studies are based on an analysis of a very limited segment of each layer, but show the potential of this type of study for rapid qualitative identification of minerals.

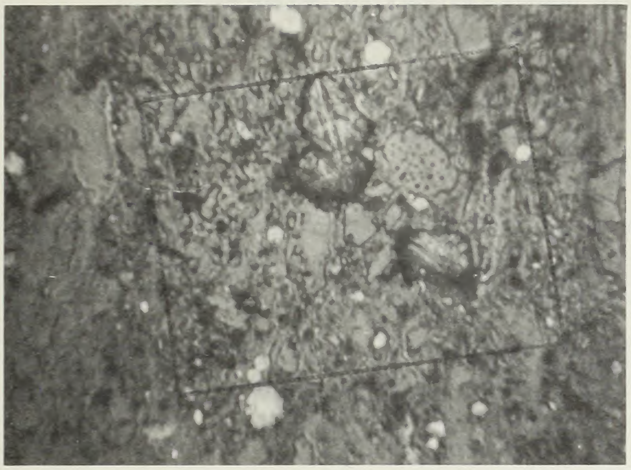

Fig. 9a. Photomicrograph showing crystals on surface of sample CMB-8-JMW-OS-2 (500x). Photo is mirror image of electron microprobe photos.

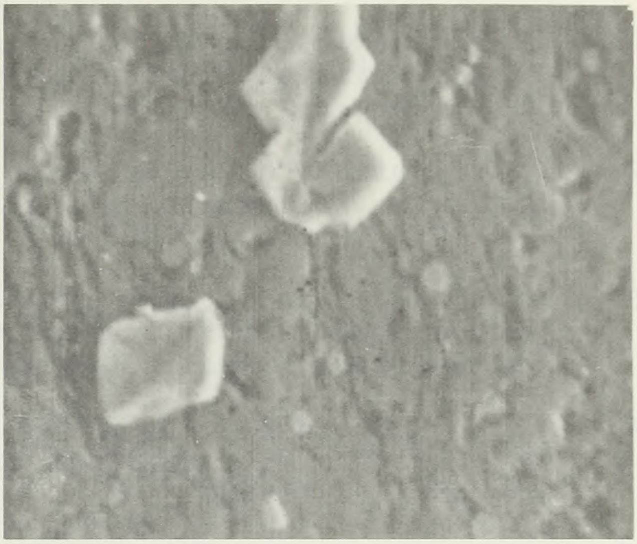

Fig. 9b. Scanning electron micrograph showing cubic nature of crystals shown in Fig. 9a (1000x).

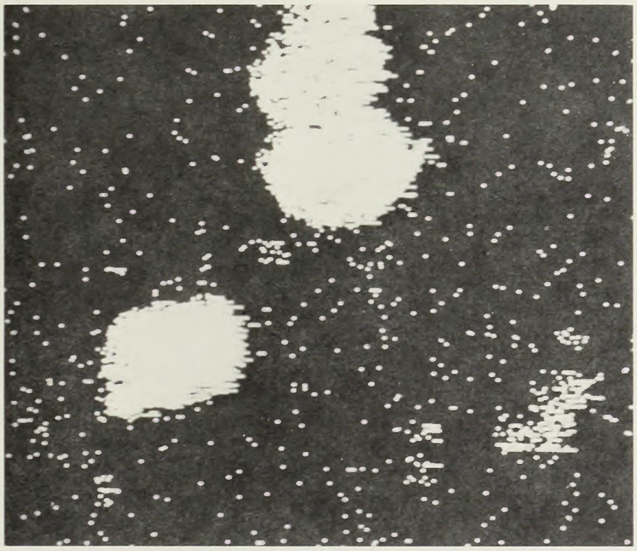

Fig. 9c. Na Kα x-ray intensity distribution, same area as shown in Fig. 9b (1000x).

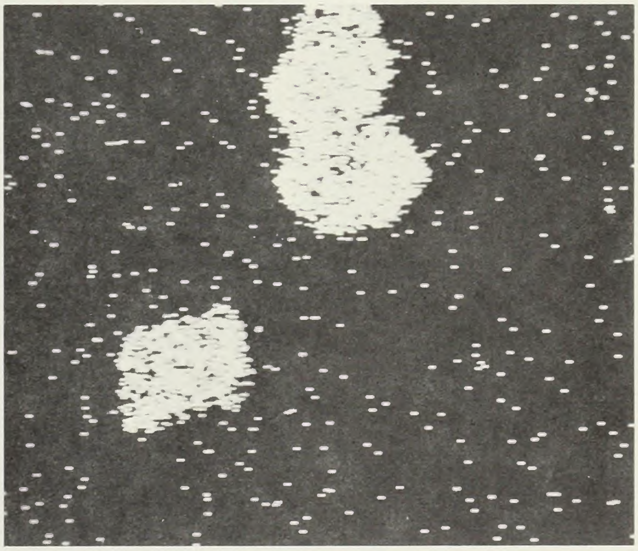

Fig. 9d. Cl Kα x-ray intensity distribution, same area (1000x).

REFERENCES

1. C. R. Knowles, J. V. Smith, A. E. Bence, and A. L. Albee, "X-Ray Emission Microanalysis of Rock-Forming Minerals. VII. Garnets, " J. Geol. 77, 439-451 (1969).

2. J. V. Smith, "X-Ray Emission Microanalysis of Rock-Forming Minerals. Clinopyroxenes Near the Diopside-Hedenbergite Join," J. Geol. 74, 463-477 (1966).

3. A. L. Albee and L. Ray, "Correction Factors for Electron Probe Microanalysis of Silicates, Oxides, Carbonates, Phosphates, and Sulfates," Anal. Chem 42, 1408-1414 (1970).

4. A. E. Bence and A. L. Albee, "Empirical Correction Factors for the Electron Microanalysis of Silicates and Oxides," J. Geol. 76, 382-403 (1968).

5. J. W. Smith, "Geochemistry of Oil-Shale Genesis in Colorado's Piceance Creek Basin," Rocky Mountain Association of Geologists, 1974 Guidebook, pp. 71-79.

6. R. G. Hurley and E. W. White, "New Soft X-Ray Method for Determining the Chemical Forms of Sulfur in Coal," Anal. Chem. 46, 2234-2237 (1974).

☆ US GOVERNMENT PRINTING OFFICE: 1976—677-343/176

Form 1279—3
(June 1984)

BORROWER'S C

QE 471 .S5 H35 1976 c.

Electron microprobe st
of Mahogany zone and

DATE LOANED	BORROWER

USDI — BLM

AREA OIL SHALE OFFICE
CENTRAL LIBRARY